Supporting Information

Enhanced Raman sensitivity and magnetic separation for urolithiasis detection using phosphonic acid-terminated Fe_3O_4 nanoclusters.

Yi-Chun Chiu[1], Po-An Chen[2], Po-Yang Chang[2], Cheng-Yang Hsu[2], Ching-Wei Tao[3], Chih-Chia Huang[2,3,5], and Huihua Kenny Chiang[2,3,4*]*

[1]Division of Urology, Department of Surgery, Zhong Xiao Branch, Taipei City Hospital, Taipei, Taiwan

[2] Institute of Biophotonics, National Yang-Ming University, Taipei, Taiwan

[3] Institute of Biomedical Engineering, National Yang-Ming University, Taipei, Taiwan

[4] Biophotonics and Molecular Imaging Research Center (BMIRC), National Yang-Ming University, Taipei, 112, Taiwan

[5] Department of Photonics, Center for Micro/Nano Science and Technology, and Advanced Optoelectronic Technology Center, National Cheng Kung University, 701, Tainan, Taiwan.

Email: c2huang@mail.ncku.edu.tw; hkchiang@ym.edu.tw

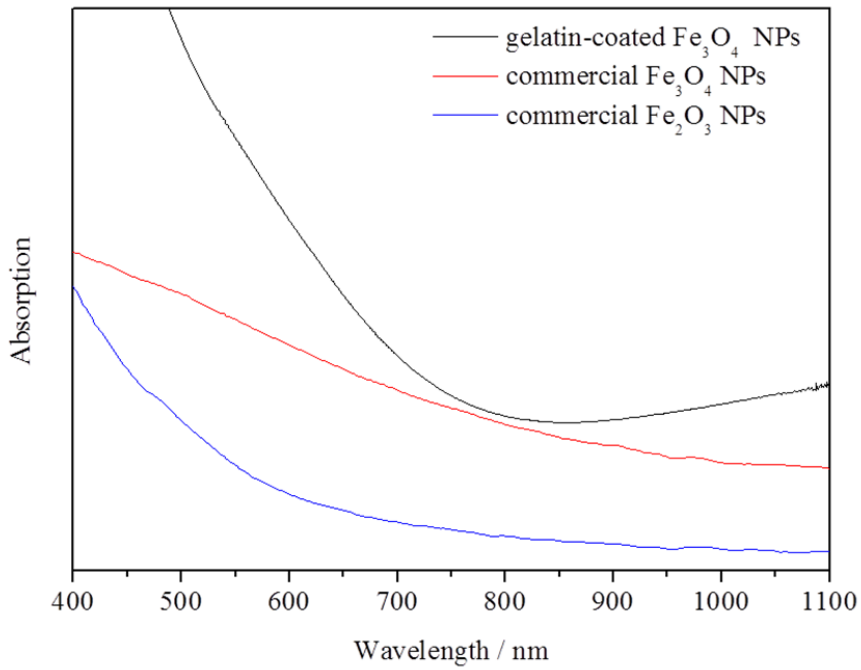

Figure S1. UV-visible spectra of gelatin-coated Fe_3O_4 NPs, commercial Fe_3O_4 NPs (Alfa Aesar; 20-30 nm), and Fe_2O_3 NPs (Sigma-Aldrich; < 50 nm).

Figure S2a shows a FT-IR spectrum of gelatin-coated Fe_3O_4 nanoclusters. A band at 570 cm^{-1} is consistent with the Fe–O vibrations of the Fe_3O_4 structure.[1] The absorptions at 1633 cm^{-1}, 1548 cm^{-1}, 1263 cm^{-1} were assigned to amide I (1600−1690 cm^{-1}, C=O stretching), amide II (1480−1575 cm^{-1}, CN stretching, NH bending), and amide III (1229−1301 cm^{-1}, CN stretching, NH bending) from gelatin molecule. Peaks at 1580 cm^{-1} and 1425 cm^{-1} are due to the presence of $\nu as(COO)^-$ and $\nu s(COO)^-$, respectively,[1,3] from organic gelatin, citrate, and TMA molecules capped onto the surface of the Fe_3O_4 nanoclusters. A broaden band coupled with peaks at 952 cm^{-1} and 860 cm^{-1} is possible related to γ(O-H • • O) and δ(C–O) groups.[3]

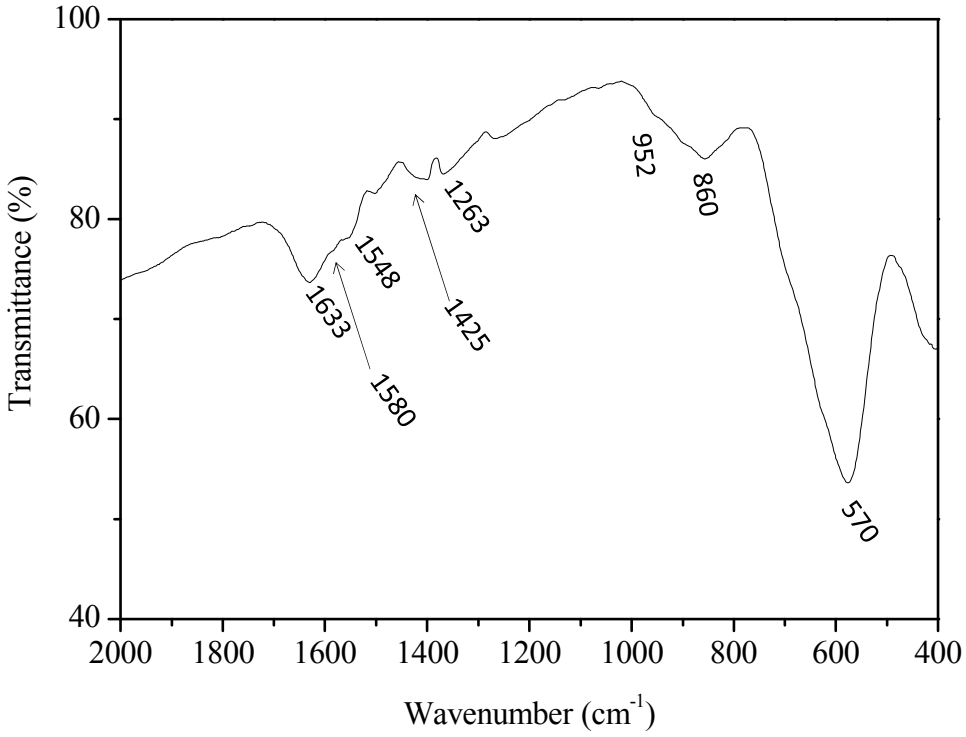

Figure S2. FT-IR measurement of as-prepared gelatin-coated Fe_3O_4 nanoclusters.

References

1. G. V. M. Jacintho, A. G. Brolo, P. Corio, P. A. Z. Suarez, and J. C. Rubim, *J. Phys. Chem. C*, **2009**, *113*, 7684.
2. J. Banker, *Biochim. Biophys. Acta*, **1992**, *1120*, 123.
3. Filipe A. Almeida Paz and Jacek Klinowsk, *Inorg. Chem.,* **2004**, *43*, 3882

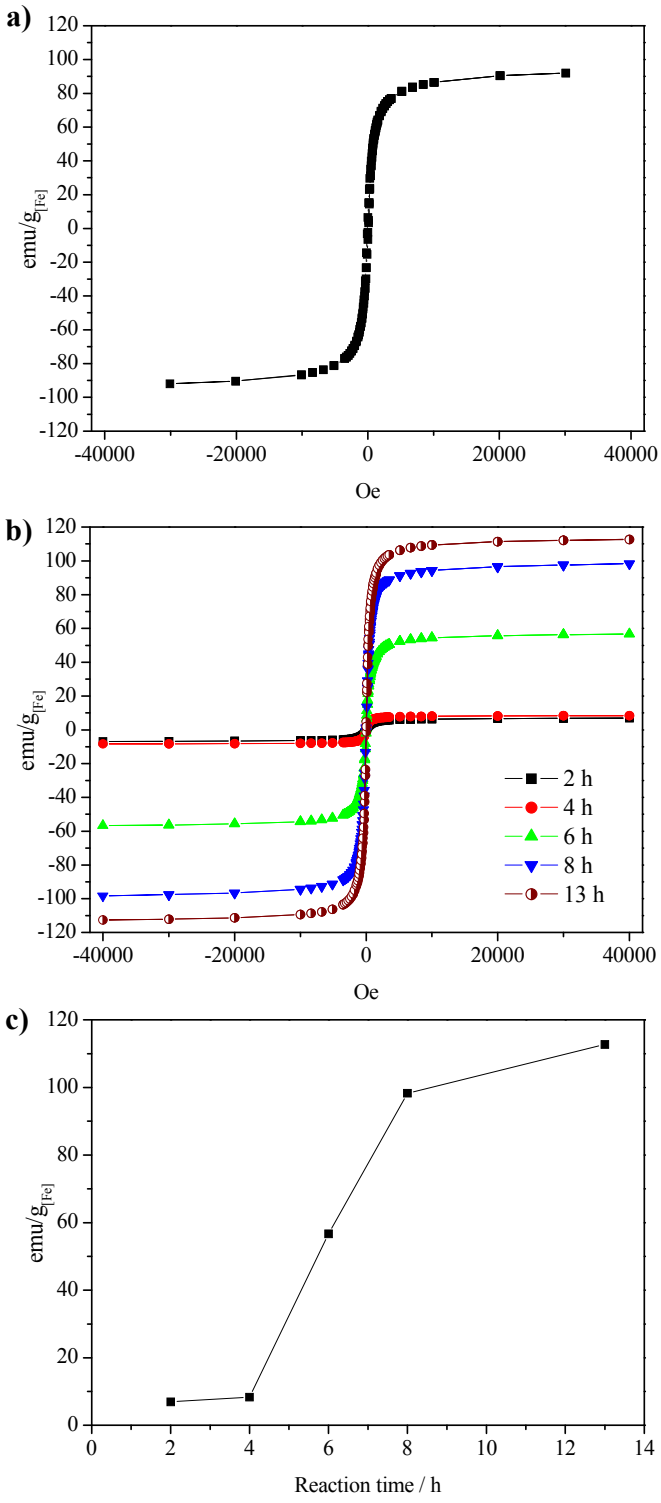

Figure S3. a) SQUID measurements of M-H plot (300K) of N_2H_4/gelatin-free Fe_3O_4 nanoparticles. SQUID measurements of b) M-H plot (300 K) and c) Ms value-reaction time plot of as-synthesized Fe_3O_4 nanoclusters obtained at different reaction time.

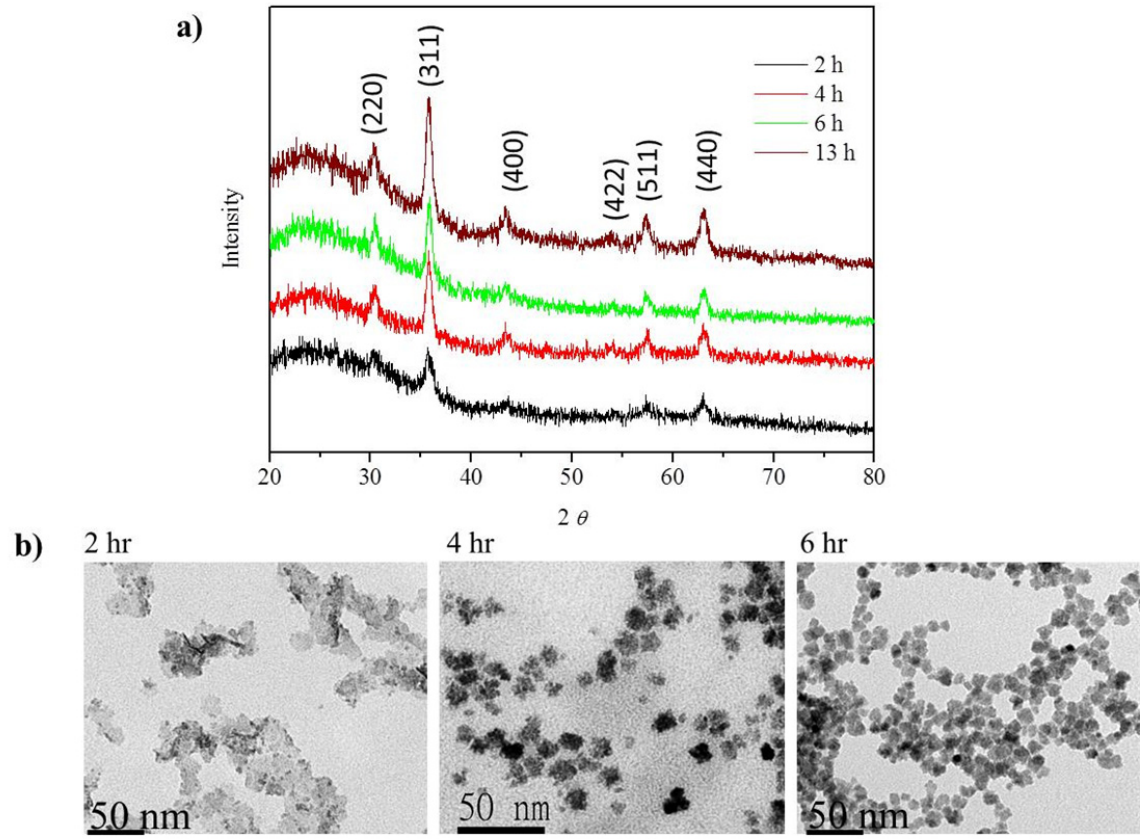

Figure S4. Time-dependent a) XRD patterns and b) TEM images of gelatin-coated Fe_3O_4 nanoclusters prepared at different reaction times.

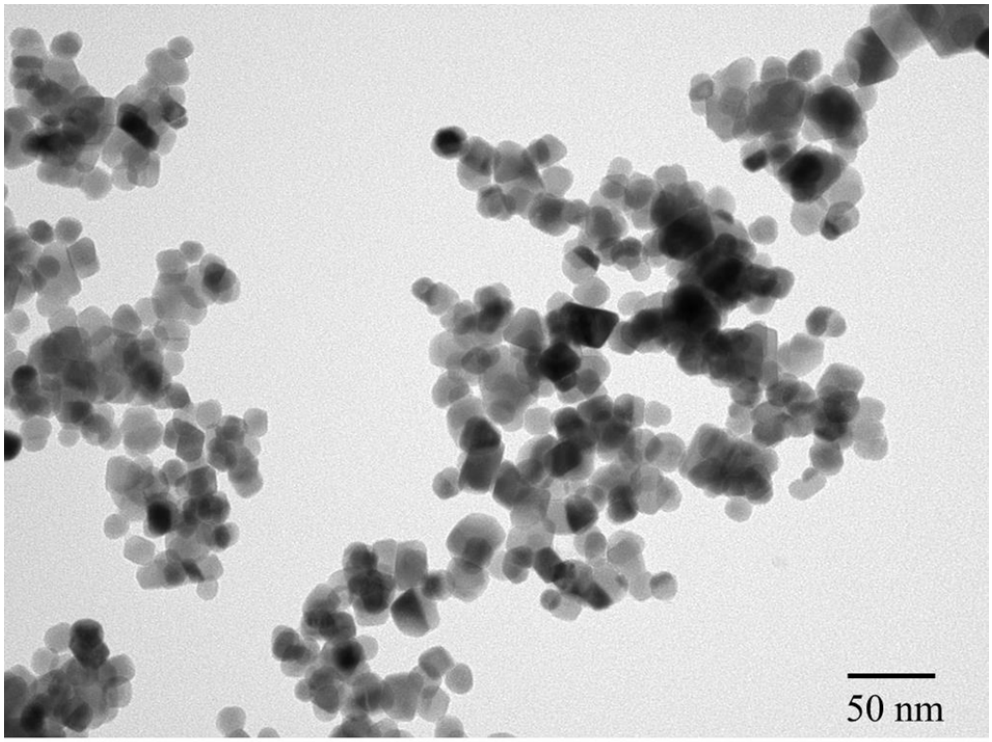

Figure S5. TEM image of gelatin-free Fe_3O_4 nanoclusters.

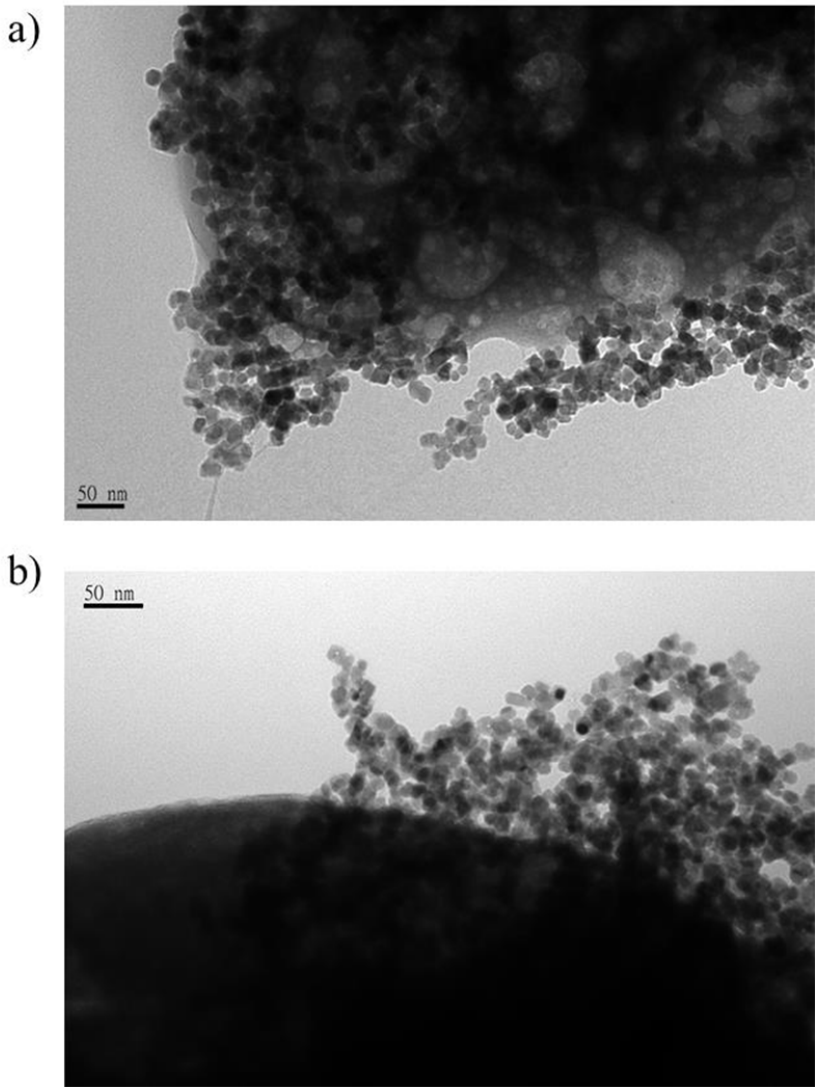

Figure S6. TEM images of Fe_3O_4 nanoclusters coating on the surface of a) COD and b) COM crystals.

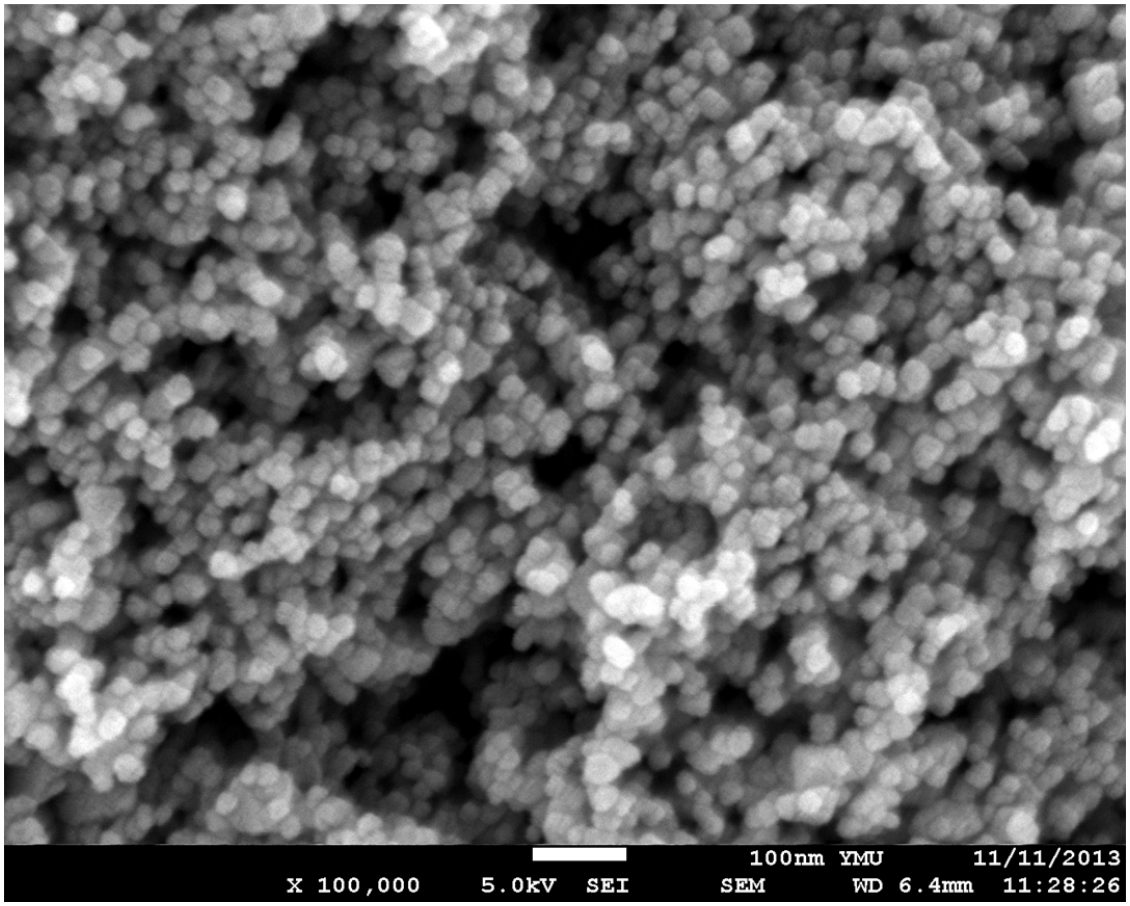

Figure S7. SEM images of gelatin-coated Fe_3O_4 nanoclusters deposited on the surface of a Si wafer.

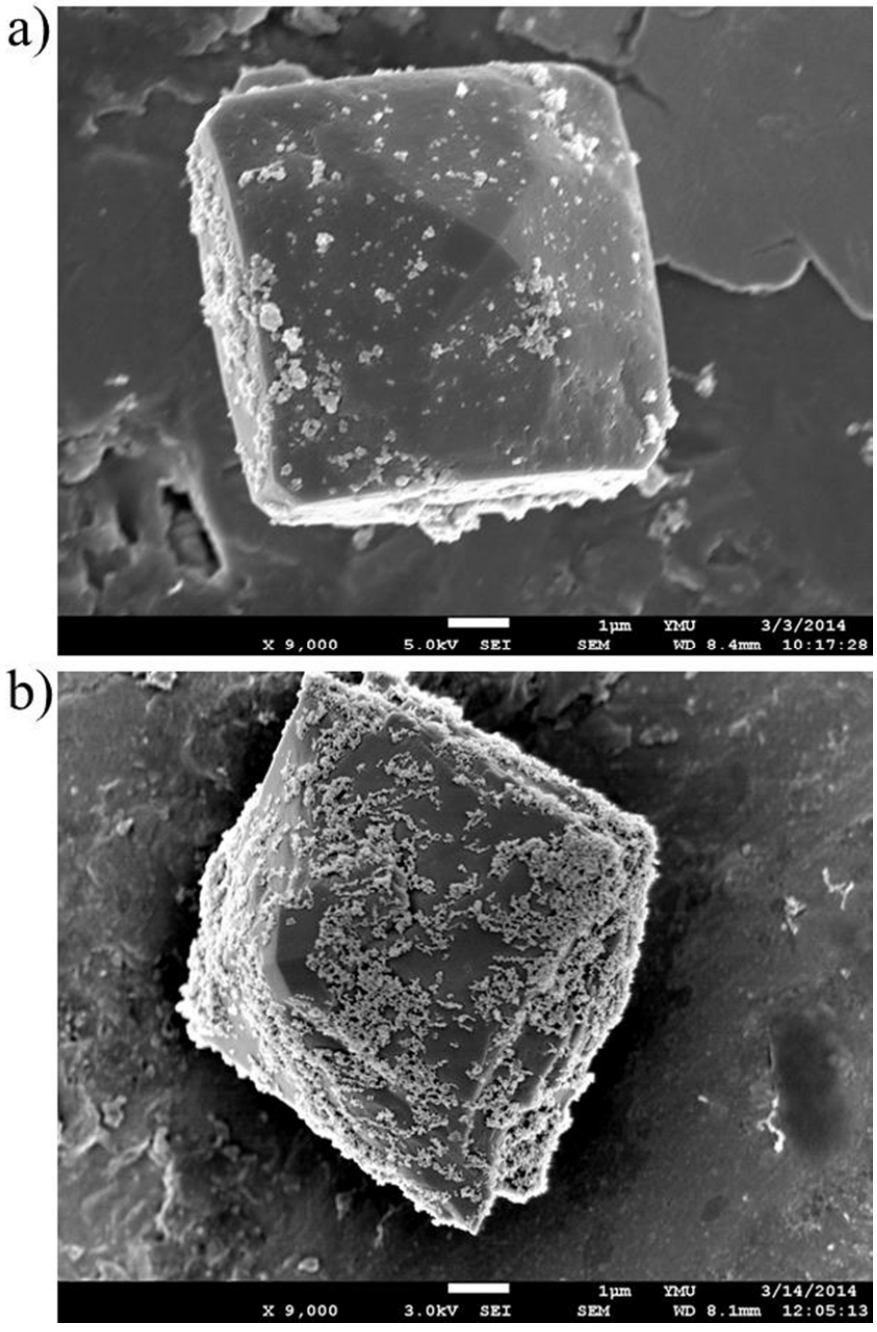

Figure S8. SEM images of a) gelatin-coated Fe_3O_4 nanoclusters and b) phosphonic acid-terminated Fe_3O_4 nanoclusters attached to the surface of COD crystals.

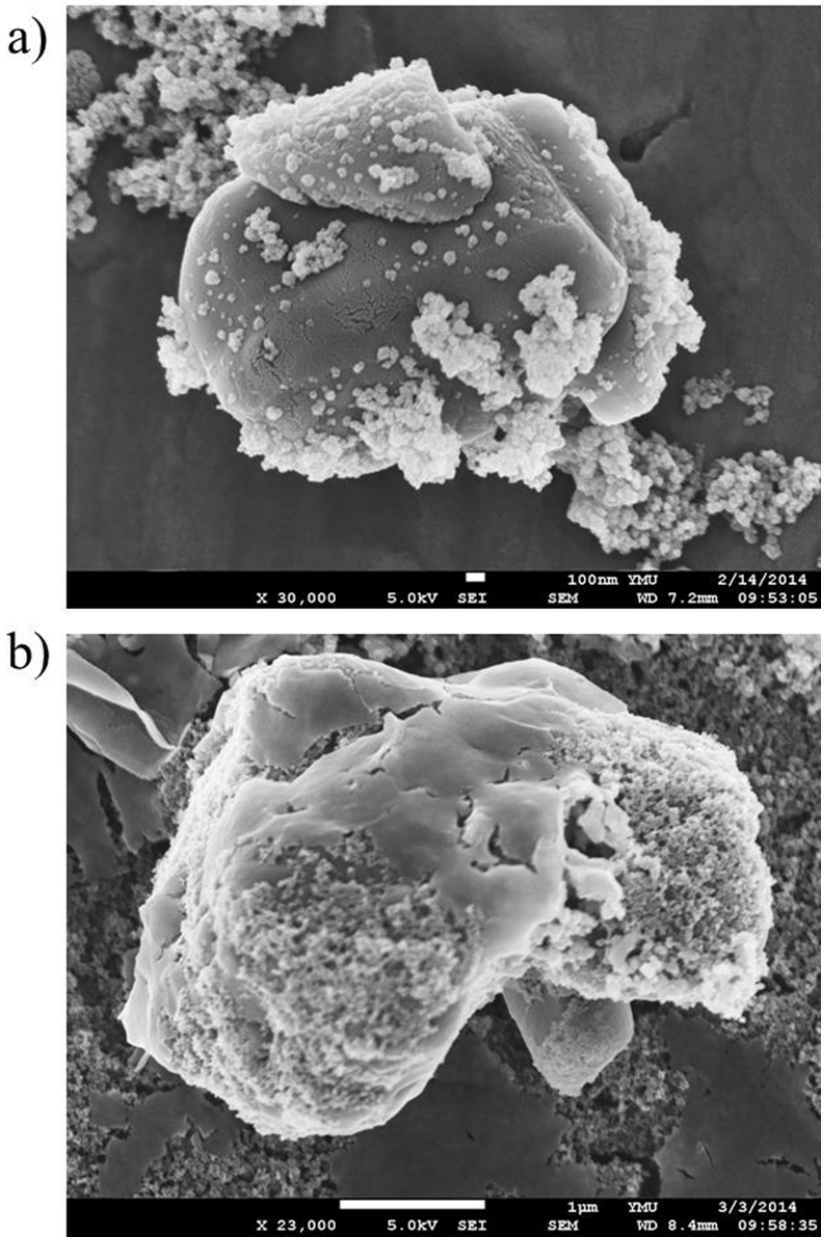

Figure S9. SEM images of a) gelatin-coated Fe_3O_4 nanoclusters and b) phosphonic acid-terminated Fe_3O_4 nanoclusters attached to the surface of COM crystals.

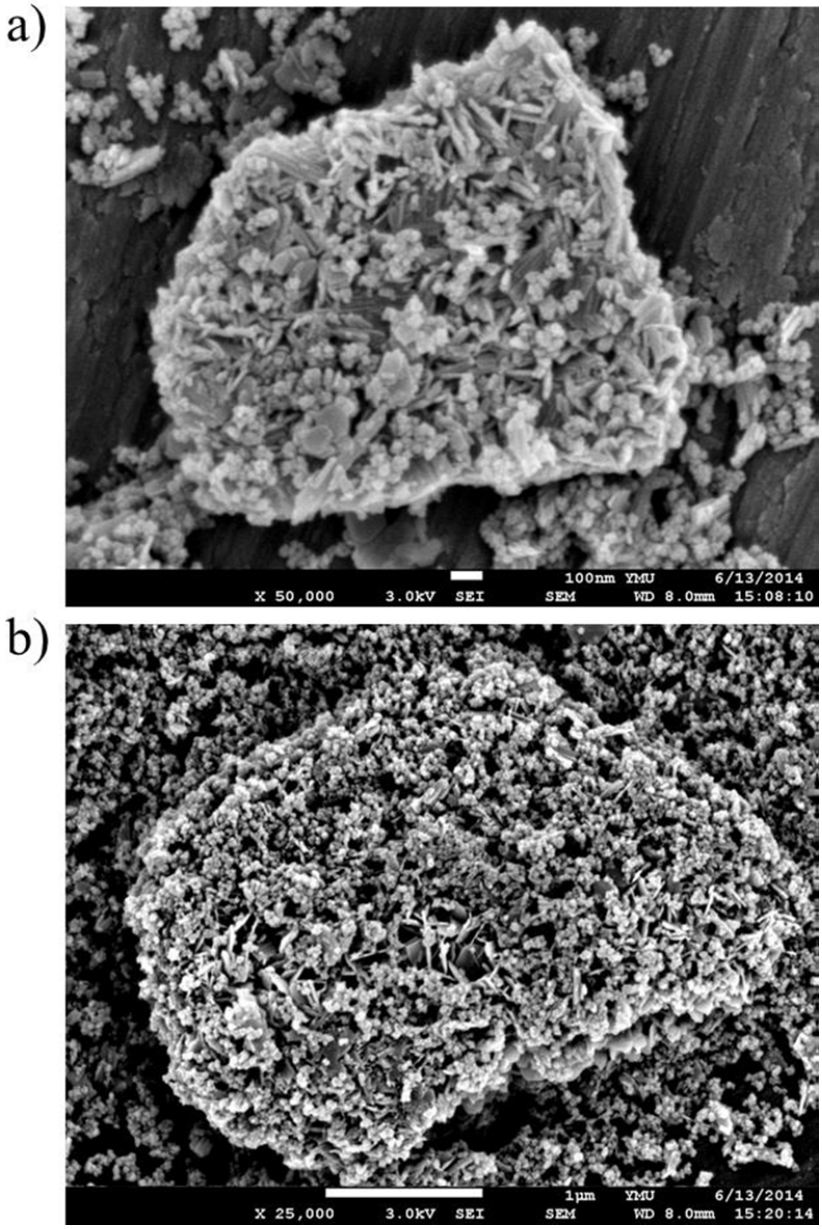

Figure S10. SEM images of a) gelatin-coated Fe_3O_4 nanoclusters and b) phosphonic acid-terminated Fe_3O_4 nanoclusters attached to the surface of HAP crystals.

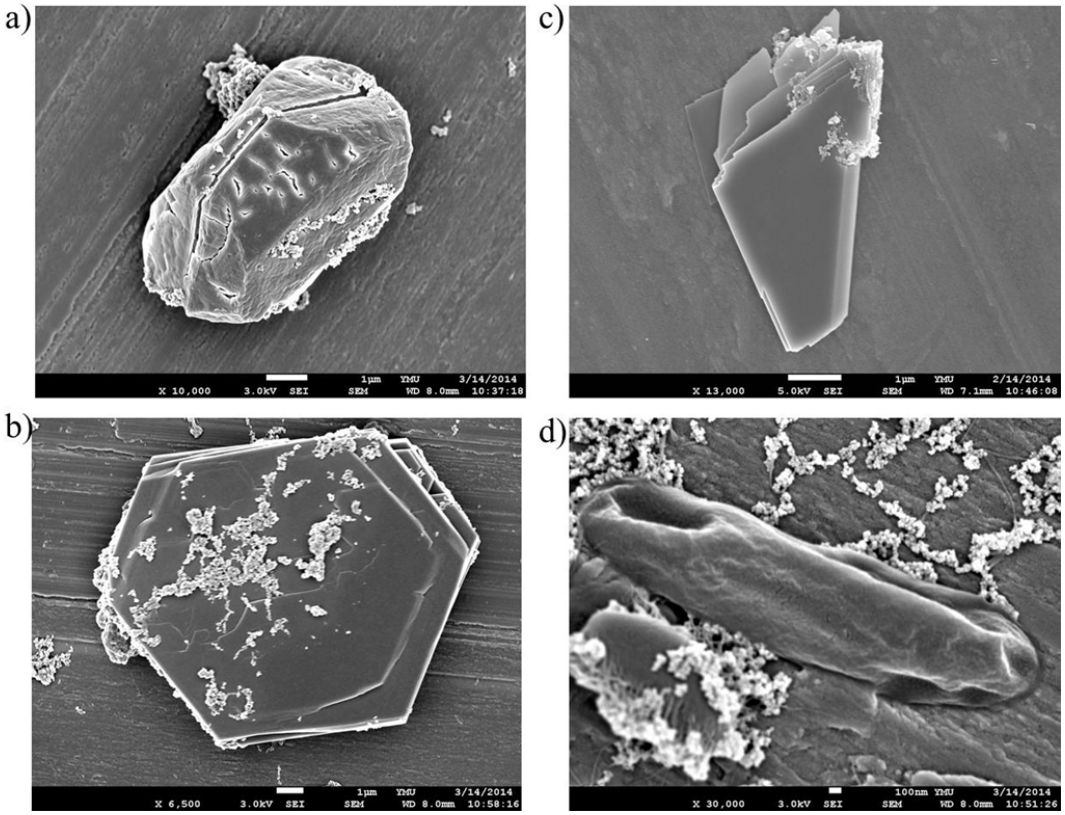

Figure S11. SEM images of gelatin-coated Fe_3O_4 nanoclusters attached to the surface of a) MG, b) Cys, c) DCPD, and d) UA crystals.

Because the regular geometry of COD crystals favored a theory measurement, we calculated the coating density of phosphate terminal Fe_3O_4 nanoclusters on a COD crystal using Matlab software (Figure S11). The bright contrast was mapped to calculate the total areas of Fe_3O_4 nanoclusters in the 1/8 surface of a COM crystal, including a triangle and a rectangle block. We assumed each particle of the Fe_3O_4 nanocluster consisted of three Fe_3O_4 nanocrystals, leading to a contribution of ~ 40 nm in height. As a result, a rough estimation gave approximately 3.44 x 10^6 Fe_3O_4 NPs anchored to a single COD crystal.

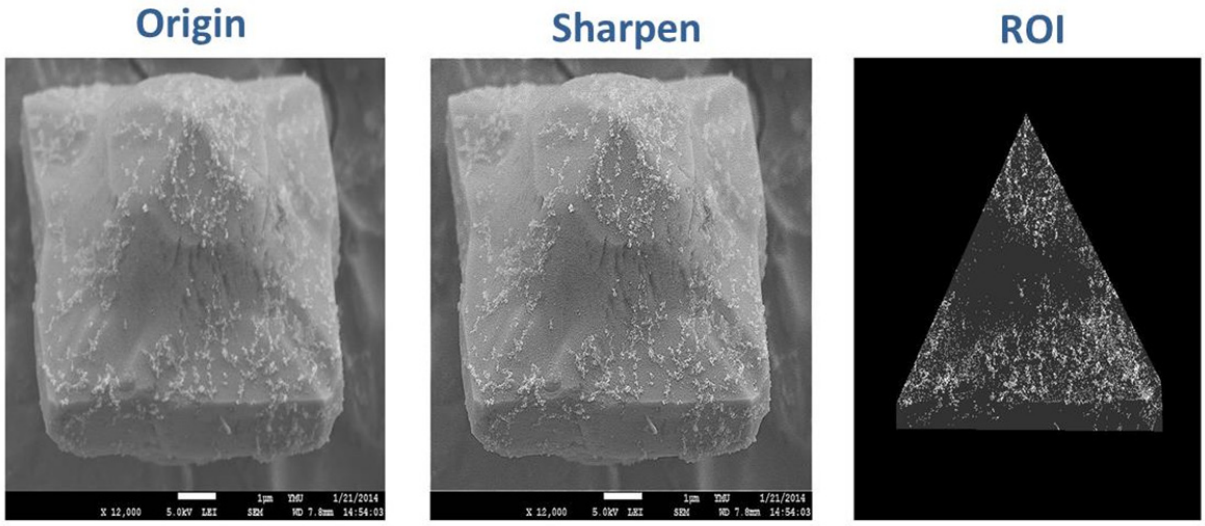

Figure S12. Imaging analysis of the coverage of phosphonic acid-terminated Fe_3O_4 nanoclusters onto a single COD crystal, followed with treatment of imaging sharpening (middle) and ROI selection (right) for the quantitative calculation of brightening spots in the ROI area, which was performed using a Matlab algorithm.

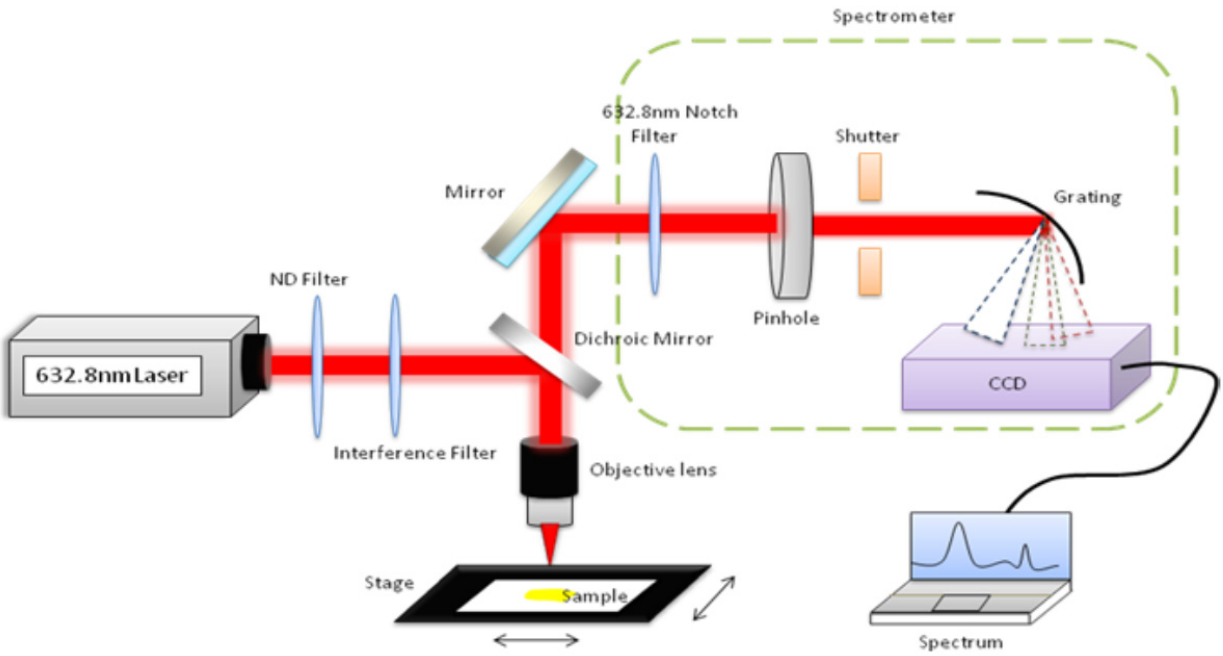

Figure S13. Illustration of our custom-built Raman spectroscope system equipped with a 632.8 nm laser.

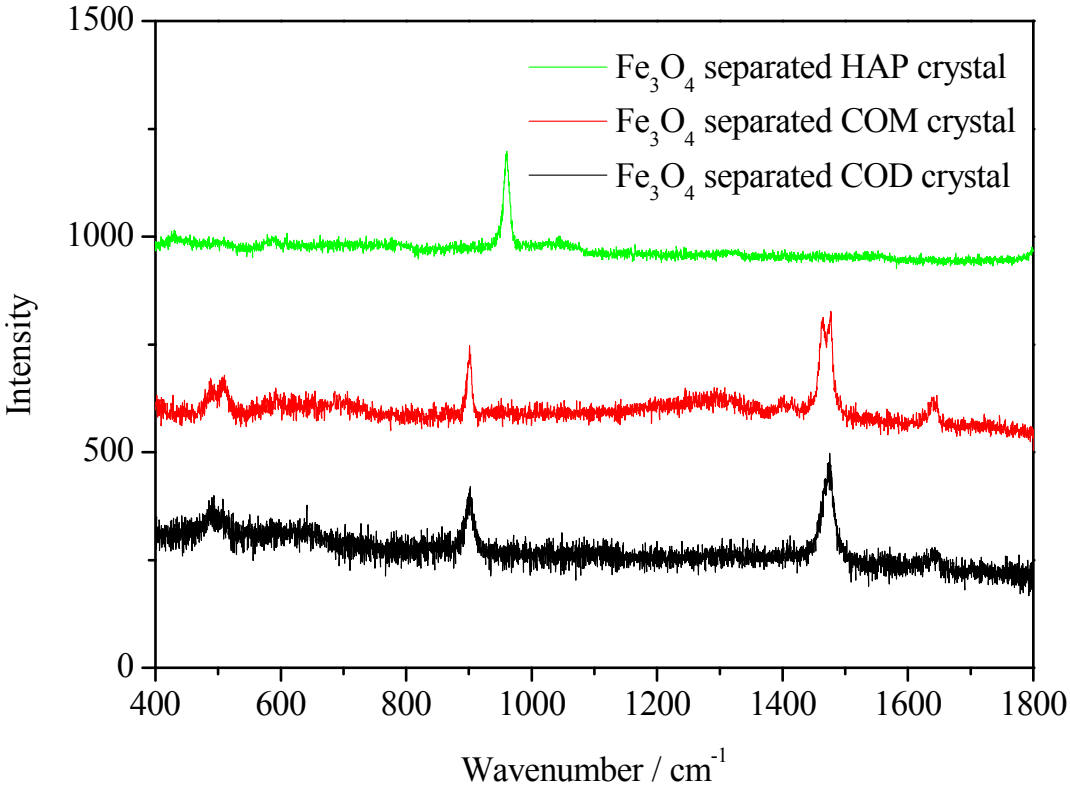

Figure S14. Raman spectra of Fe_3O_4-COD, Fe_3O_4-COM and Fe_3O_4-HAP, where the Ca-based samples were used from standard powders.

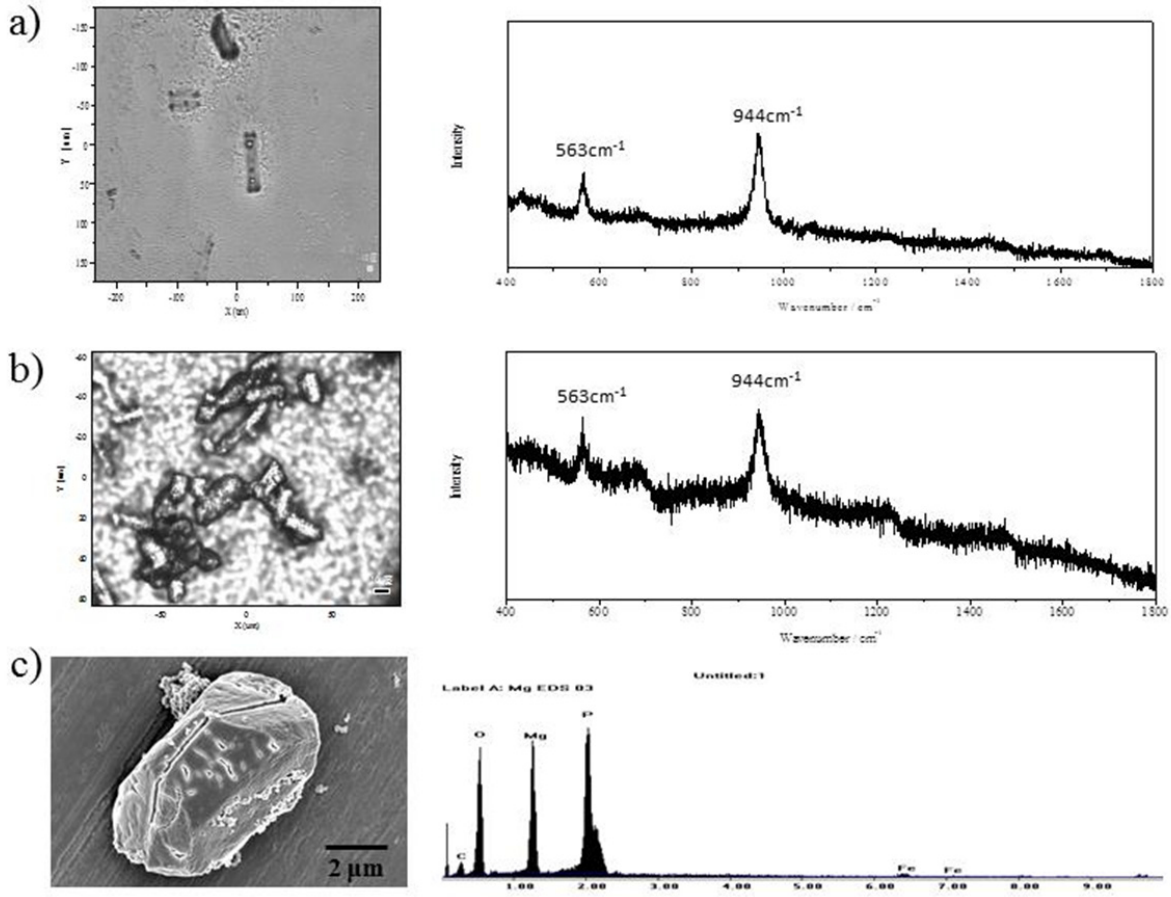

Figure S15. Optical image and Raman spectra of struvite crystals before a) and after b) binding with phosphonic acid-terminated Fe_3O_4 nanoclusters. c) SEM and EDS measurements of struvite crystals after binding with phosphonic acid-terminated Fe_3O_4 nanoclusters.

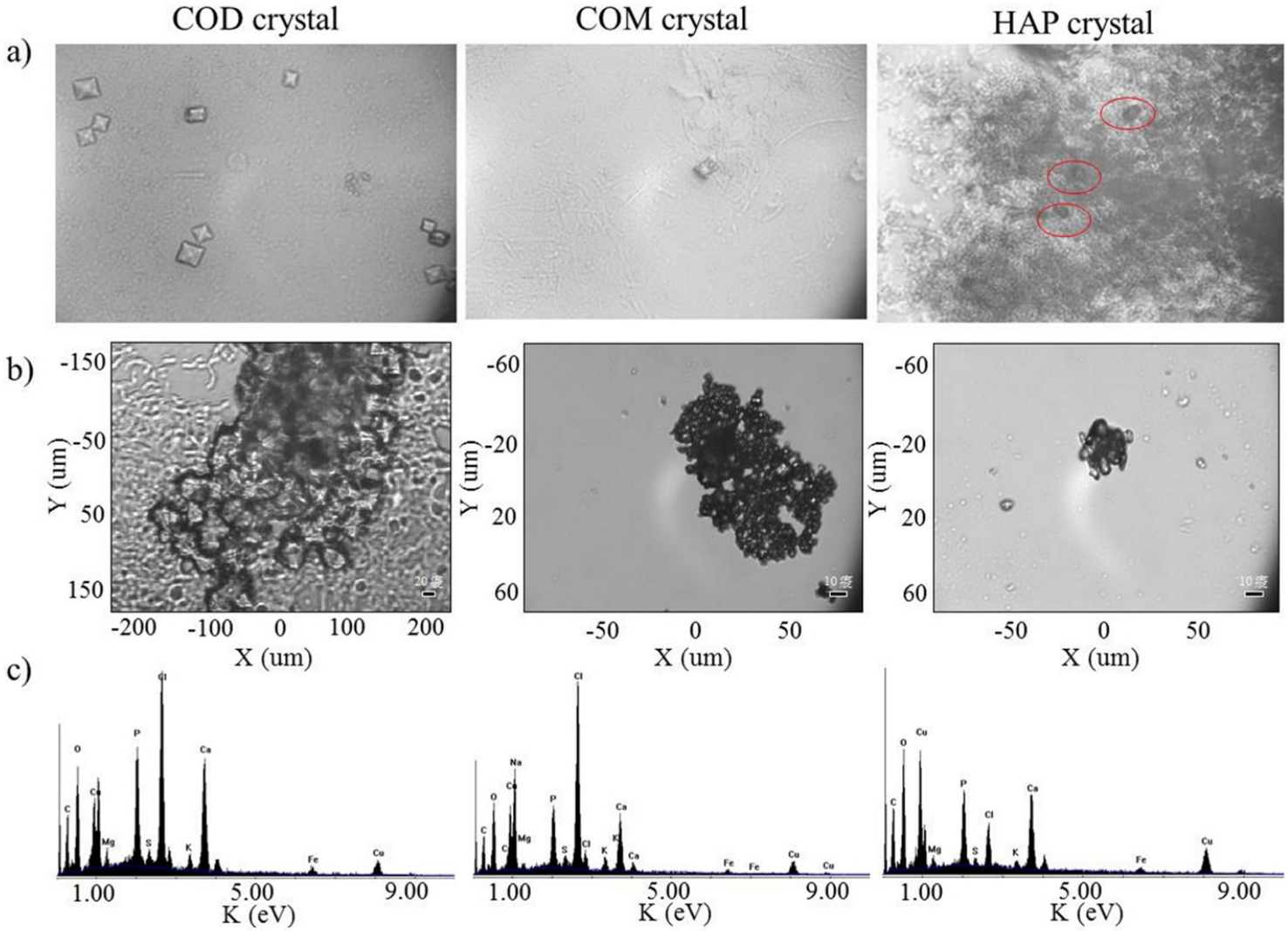

Figure S16. Bright-field images of urinary crystals with a) physical collection and b) magnetic collection with phosphonic acid-terminated Fe_3O_4 nanoclusters. c) EDS measurements of the phosphonic acid-terminated Fe_3O_4 nanoclusters-urinary crystals.